

Dose sensitivity of MAGIC-f polymer gel using different MRI sequences

Cavedini^a N.G., Papaléo^{a,b} R.M., Jobim^a N.B., Schuck^c P.N., Garrafiel^d F.N.,
Oliveira^b E.M.N. de, Schwarcke^e M.M.B., Oliveira^f A.C.H.,
Caribé^g P.R.R.V., Marques da Silva^{a,h} A.M.M.

^aMedical Image Computing Laboratory (MEDICOM), PUCRS, 90619-900, Porto Alegre, RS, Brazil;

^bInterdisciplinary Center of Nanoscience and Micro-Nanotechnology, PUCRS, 90619-900, Porto Alegre, RS, Brazil;

^cDepartment of Radiology, Weill Cornell Medical College, 10021, New York, NY, United States of America;

^dHospital São Lucas, PUCRS, 90619-900, Porto Alegre, RS, Brazil;

^eDepartment of Exact and Social Applied Sciences, UFSCPA, 90050-170, Porto Alegre, Brazil;

^fFaculdade Nova Esperança, 58067-698, João Pessoa, PB, Brazil;

^gMedical Imaging and Signal Processing (MEDISP), Ghent University, 9000, Ghent, Belgium.

^hMedical Imaging & Data Analytics (MEDIIMA), 92107, San Diego, CA, USA.

nicollas.cavedini@acad.pucrs.br

ABSTRACT

This study aims to evaluate the dose sensitivity of MAGIC-f gel irradiated by high-energy photon beams, comparing quantification using different MRI sequences. Irradiation was performed using 6 MV photons with 600 cGy/min dose rate, field size of 20x20 cm², and 94 cm source-to-surface distance. Two gel batches were produced on different days and placed in vials. In the first batch, doses of 0, 2, 4, 6, 8, 10, 20, and 40 Gy were planned. The second batch was irradiated with doses of 0, 2, 4, 6, 10, 12, 14, and 16 Gy. MR images were acquired with Spin Echo (SE, TR=3 s) and Multi Spin Echo (MSE, TR = 3s or 10s, turbo factor 24) sequences. The dose is assessed via changes in the transverse relaxation time in the irradiated gel. In MSE, dose sensitivity in the first batch was 0.27 (TR=3 s) and 0.28 Gy⁻¹s⁻¹ (TR=10 s) and in the second batch, 0.31 and 0.31 Gy⁻¹s⁻¹ (TR = 3 s and TR = 10 s, respectively). In the SE sequence, dose sensitivity was 0.42 for the first batch and 0.43 Gy⁻¹s⁻¹ for the second batch. Linearity of dose-response was only obtained for doses below 10 Gy. Comparing the dose sensitivity extracted from MSE and SE sequences using TR= 3s, differences around 30% were found. Thus, although MSE-MRI offers a faster protocol of imaging acquisition it is less precise for quantification of relaxation times, as TE is not a well-defined quantity. The performance of the gel as a dosimeter is consequently sequence dependent.

Keywords: dosimetric gel, MAGIC-f, 3D dosimetry, magnetic resonance, spin echo.

1. INTRODUCTION

Gel dosimetry is a technique based on water radiolysis, triggering chemical changes in the gel associated with an absorbed dose of ionizing radiation [1]. The advantage of polymer gels as dosimeters is the ability to extract information about the absorbed dose in three dimensions (3D), since polymerization is retained at the radiation interaction point. 3D dosimetry is an excellent technique for radiotherapy quality assurance, as in IMRT (intensity-modulated radiation therapy) [2].

The polymeric gel MAGIC (Methacrylic and Ascorbic acid initiated by copper) is a type of nMAG (Normoxic Methacrylic Acid Gel), more accessible to manufacture and produce on a laboratory bench under an oxygen atmosphere due to the presence of ascorbic acid in its formulation, an antioxidant [1]. Previous studies introduced formaldehyde in MAGIC gel composition [3]. MAGIC-f shows an increase in dose sensitivity and gel melting temperature, and the formaldehyde does not intervene in the chemical reactions that ionizing radiation induces in the gel. In addition, the increase of the melting temperature allows the gel to become stable at higher temperatures.

Several imaging techniques have been used to extract the dose quantification in polymer gels, such as ultrasound [4], Computed Tomography (CT) [5], and Magnetic Resonance Imaging (MRI) [6]. Polymer gel dosimetry associated with MRI has an advantage over CT due to the absence of ionizing radiation. The image acquisition in MR does not affect the changes of the polymeric chains induced by the irradiation. The dose quantification using MRI is possible because when ionizing radiation creates long polymeric chains in the gel, water mobility is reduced, changing the transverse relaxation times of protons, T₂. Thus dose-response curves can be produced from T₂-weighted images, associating the variation in T₂ (or R₂=1/T₂) values with the absorbed dose. Although MRI is considered the gold standard for dose quantification in gel dosimetry, it is important to choose the MR imaging sequence that will suit the best in the clinical environment to develop an optimized acquisition protocol [1,6]. This study aims to evaluate the dose sensitivity of polymer gel MAGIC-f exposed to a high-energy photon beam, comparing the response of Multi Spin-Echo (MSE) and Single Spin-Echo (SE) MRI sequences.

2. MATERIALS AND METHODS

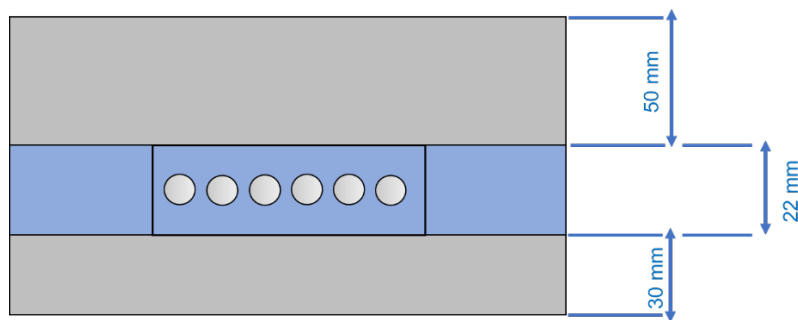
2.1. Gel production

100 mL of MAGIC-f dosimetry gel were prepared with 82 mL of milli-Q water, 8.2 g of 300 Bloom swine gelatin, 0.67 mL of copper sulfate pentahydrate, 3 mL of formaldehyde stabilized in 37% methanol, 5.9 mL methacrylic acid, and 35.2 mg ascorbic acid [7]. Milli-Q water was first heated up to 50°C. The heating was then turned off, keeping the magnetic stirrer on. Gelatin was added slowly until the solution got homogeneous. Sequentially, the copper sulfate pentahydrate, ascorbic acid, methacrylic acid, and formaldehyde were added. After 5 minutes of blending when the solution became homogeneous, MAGIC-f polymer gel was ready to be placed in the vials. All vials were stored in a refrigerator for 24 hours before irradiation.

2.2. Phantom and irradiation planning

In this study, calibration curves were acquired using vials filled with MAGIC-f. The vials were made of glass, with an inner radius, outer radius, and height of 0.45 cm, 0.55 cm, and 7.5 cm, respectively. All vials were filled to prevent oxygen contact and sealed with Parafilm®. For the irradiation experiments, a holder was manufactured from PMMA (density of 1.18 g/cm³), with a series of holes to fasten the vials. Figure 1 shows a cross-sectional view of the holder, with the radiation beam coming from the top. The vials are represented as circles inside the acrylic, represented in blue. On top of the acrylic holder, a 50 mm solid water plate (in gray) was placed to ensure appropriate dose build-up. At the bottom, another solid water plate (in gray) with a 30 mm thickness was positioned to provide backscattering. Planning CT of the phantom and vials were acquired using Philips® Ingenuity 64-channel scanner. CT images were exported to the Eclipse® Varian treatment planning system (Varian Medical Systems, Palo Alto, CA). A marker was placed at the phantom center, positioning the isocenter point for radiation planning.

Figure 1: Scheme of the irradiation sample holder, with the sample vials (circles) inside the PMMA plate (blue) between solid water (gray). Both sides of the holder had blocks of acrylic. The central area can be removed to insert the vials.



2.3. Irradiation

All irradiations were performed using a 6 MV photon beam from a Varian IX (Varian Medical Systems, Palo Alto, CA) linear accelerator with 600 cGy/min of dose rate, 20 x 20 cm² beam field size, and 94 cm source-to-surface distance (SSD). During irradiation, the gantry was positioned at 0°. The setup positioning was verified using lasers in the treatment room to ensure the same irradiation position on the table. All MAGIC-f gel batches were stored in the refrigerator at 5°C controlled temperature before the irradiation. Irradiation was performed at least 24 h after the synthesis of the gel.

For the irradiation of the first batch, doses of 0 (control), 2, 4, 6, 8, 10, 20 and 40 Gy were planned. For the second batch of samples doses of 2, 4, 6, 10, 12, and 16 Gy were employed. Different dose values were chosen to investigate the behavior of the gel at doses higher than 10 Gy. Previous studies report that the dose-response curve is linear in the dose range of 0 to 10 Gy and a saturation behavior in the response occurs for much larger doses [1,8]. To minimize the total irradiation time, six vials were positioned inside the sample holder and irradiated in 2 Gy steps. At the end of each irradiation, one vial was removed, and the process continued until the maximum dose was reached.

2.4. MRI acquisition

MR images were acquired on a GE Healthcare® Optima™ MR450w 1.5 T scanner, 48 h after irradiation at the Diagnostic Imaging Center of Hospital São Lucas, PUCRS. The irradiated samples were positioned in a circular foam phantom with holes placed at the same distance from the phantom

center. For the R2 quantitative measurement, the phantom with the vials was positioned at the center of a head coil. Images were acquired using two different T2-weighted sequences: Multi Spin Echo (MSE) and Spin Echo (SE). For the MSE sequence, two TR were employed (3 s and 10 s) and an echo train (or turbo factor) of 24. A series of images were then collected, each with a different TE (10, 20, 40, 60, 80, 100, 120, 140, 160, 180, and 190 ms). The acquisition time was 1min 16sec (TR=3 s) and 3min 51sec (TR=10 s). For the SE sequence, a TR=3 s was used and a set of 11 images were obtained using different TEs (10, 20, 40, 60, 80, 100, 120, 150, 200, 350, and 400 ms). The acquisition time in this case was 7 min for each TE. Table 1 shows the full set of parameters for both MRI sequences.

Table 1: Parameters used for the MRI acquisition.

Parameters	MSE	SE
Matrix Resolution	128x128 pixels	128x128 pixels
NEX	1	1
Pixel Bandwidth	15.63 Hz	15.63 Hz
Shim	auto	auto
Slice Thickness (mm)	5	5
FOV (mm)	300	300
Slice spacing (mm)	10	10
Eco train	24	-
N° of Slices	2	2

2.5. MRI analysis

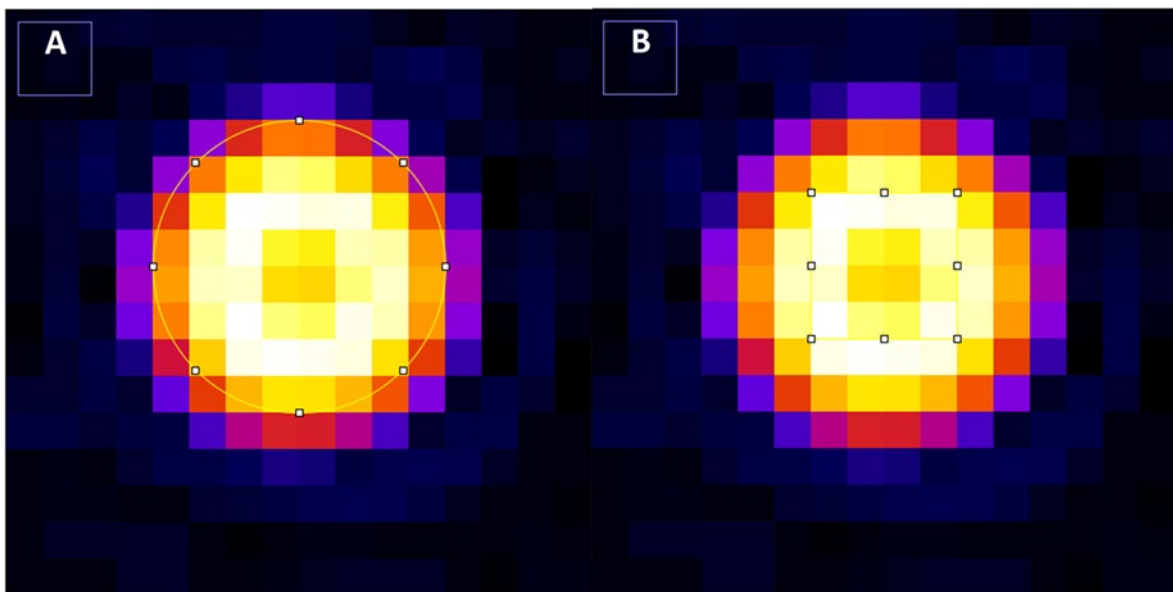
All MR images were exported to a personal computer using DICOM standards. The software ImageJ was used for image segmentation and analysis. Using the “ROI Manager” tool (Figure 2), two types of region of interest (ROI) were analyzed: 1) A circular ROI with a diameter of 8 pixels, and 2) 4 x 4 pixels positioned in the center of the vials, avoiding the vial walls. This aims to analyze the ROI influence on R2 values and dosimetry. The same ROI was applied to all the vials of each image. The average signal intensity $S(TE)$ and standard deviation in each ROI were extracted. For each irradiation dose, the signal intensity was plotted as function of TE and T2 was obtained from the fittings of the transverse relaxation Equation 1 to the data points:

$$S(TE) = S_0 e^{-TE/T_2} \quad (1)$$

The relaxation rate R2 is obtained simply using the Equation 2:

$$R2 = \frac{1}{T_2} \quad (2)$$

Figure 2: Extraction of intensity values in ImageJ's "ROI Manager" tool. A) Circular ROI; B) 4 x 4 pixels ROI.



The dose sensitivity for each batch of the MAGIC-f gel is finally obtained from the slope of the curve of R2 as a function of dose (i.e. the dose-response curve), according to previous studies [8, 9, 10, 11].

3. RESULTS

Figure 3 shows typical curves of signal intensity $S(TE)$ versus echo time obtained from the MR images of the gels irradiated at various doses. A clear exponential decay is seen in all cases, as expected. The data were fitted to Eq. (1), to obtain T2 or R2 as a free parameter. The extracted R2 values as a function of dose are shown in Figures 4, 5 and 6 for both batches of samples and the two sequences with circular and 4 x 4 pixels ROI. The dose-response is to a good approximation linear in

the region between 0 and 10 Gy. For larger doses, saturation in the R2 values is seen, in accordance with results reported previously for this class of gels [1,8].

Figure 3: a) Example of a MR image of the phantom with 8 vials irradiated with different doses. b) Signal intensity from gel samples of the second batch irradiated at different doses as a function of TE. The lines are exponential fits to the data points using Eq. (1).

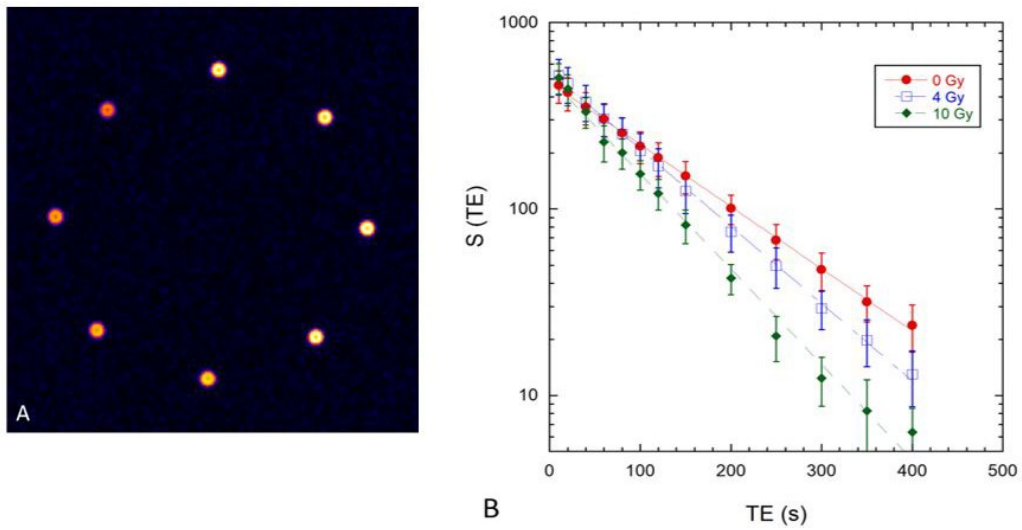


Figure 4: Dose-response curves for MAGIC-f gel using the MSE sequence using TR=3 s.

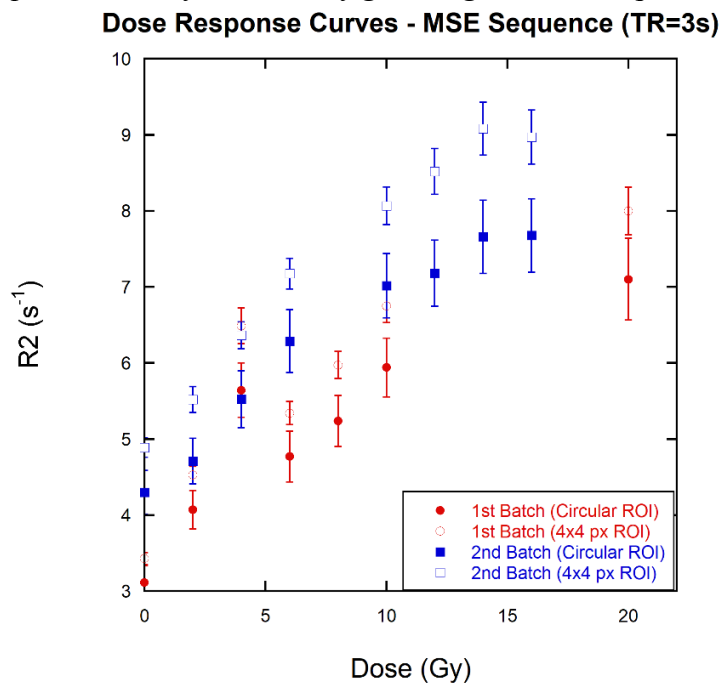


Figure 5: Dose-response curves for MAGIC-f gel using the MSE sequence using TR=10 s.

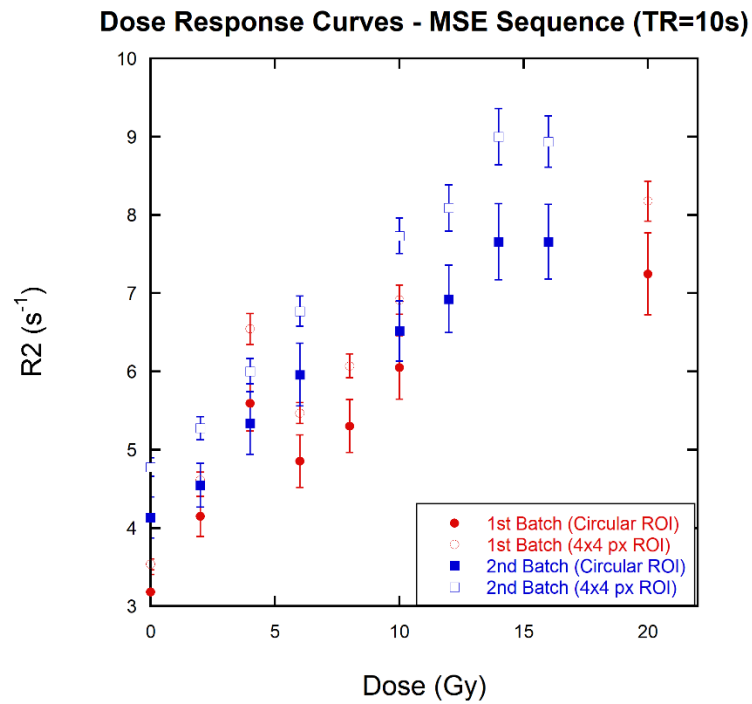
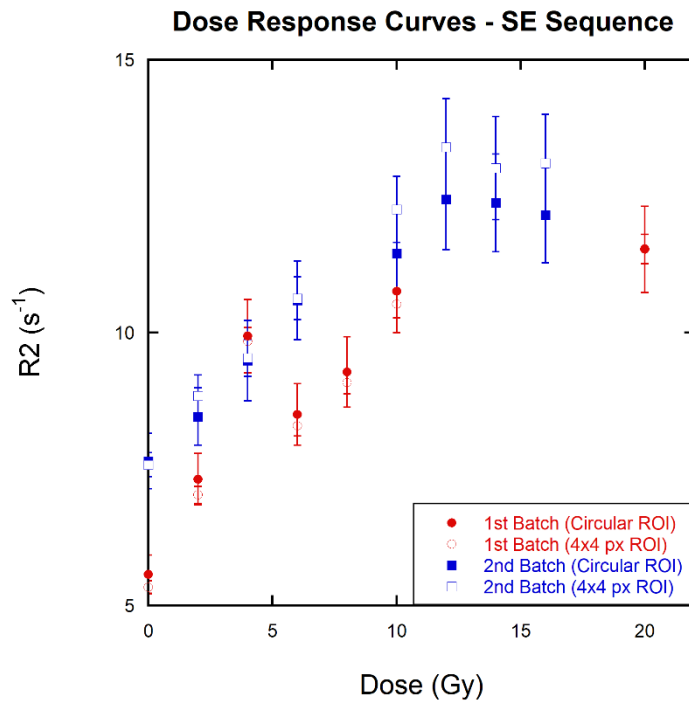


Figure 6: Dose-response curves for MAGIC-f gel using the SE sequence.



Fittings from the linear part of the dose-response curves of Figures 4, 5 and 6 allowed the extraction of the dose sensitivity parameter for each batch and acquisition sequence used. In the first batch, the vial irradiated with 4 Gy did not show the expected R2 values for both sequences. As in the second batch this problem disappeared, this result was treated as an outlier, and it was excluded from the fitting of batch 1. The Dose sensitivities values (slope of the dose-response curve) are shown in Table 2.

Table 2: Dose sensitivities ($Gy^{-1}s^{-1}$) for MSE and SE sequences using circular and 4 x 4 pixels ROI.

Type of ROI	Batch	MSE		SE
		TR=3 s	TR=10 s	TR=3 s
Circular	1st	0.23	0.23	0.41
	2nd	0.28	0.24	0.37
4x4 pixels	1st	0.27	0.28	0.42
	2nd	0.31	0.31	0.43

For the MSE sequence with TR=3 s, in the first batch, the sensitivity values of the MAGIC-f gel, were 0.27 and 0.23 $Gy^{-1}s^{-1}$, for the ROI 4 x 4 pixels and circular ROI, respectively. For the second batch, the gel sensitivity values were 0.31 and 0.28 $Gy^{-1}s^{-1}$, for the 4 x 4 pixels ROI and circular ROI, respectively. The sensitivity difference between gel batches for circular ROI is 20.06%, while for 4 x 4 pixels ROI 13.57%. For the 4 x 4 pixels ROI, sensitivity differences between the first and second batches for both TRs were close to 10%.

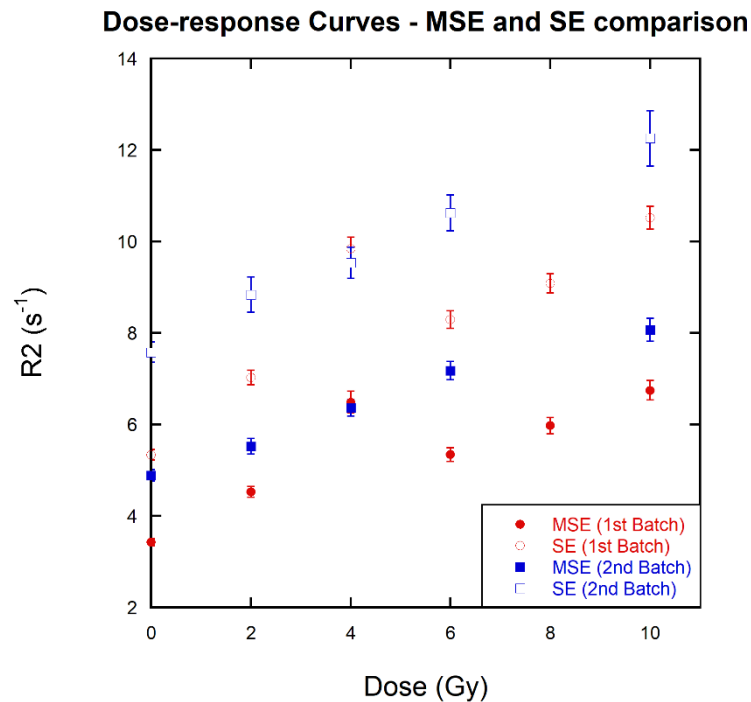
For the MSE sequence with TR= 10 s, in the first batch, the sensitivity values of the MAGIC-f gel were 0.28 and 0.23 $Gy^{-1}s^{-1}$, for the ROI 4 x 4 pixels and circular ROI, respectively. For the second batch, the gel sensitivity values were 0.31 and 0.24 $Gy^{-1}s^{-1}$, for the 4 x 4 pixels ROI and circular ROI, respectively. The sensitivity difference for circular ROI is 4.10%, while for 4 x 4 pixels ROI 8.11%.

No significant effect of the selected TR on the dose sensitivity was observed. Since the circular ROI delimitation covers the vicinity of the glass-gel interface, only the 4 x 4 pixels ROI results will be taken into account to avoid magnetic susceptibility artifacts.

Figure 6 shows the R2 dose-response for the SE MRI sequence, showing dose sensitivities of 0.42 and 0.43 $Gy^{-1}s^{-1}$, for the first and second batches. Differences between batches were even smaller in this case and within the uncertainty of the measurements.

For the SE sequence (Figure 6), in the first batch, the sensitivity values of the MAGIC-f gel, were 0.42 and 0.41 $Gy^{-1}s^{-1}$, for the ROI 4 x 4 pixels and circular ROI, respectively. For the second batch, the gel sensitivity values were 0.43 and 0.37 $Gy^{-1}s^{-1}$, for the 4 x 4 pixels ROI and circular ROI, respectively. The difference in sensitivity for circular ROI is 9.73%, while for 4 x 4 pixels ROI it is 3.56%.

Figure 7 shows the R2 dose-response curves for both MSE and SE MRI sequences (TR=3 s) in the linear regime, only considering the R2 values obtained with 4 x 4 pixels ROI. Dose sensitivity is much more influenced by the type of MRI acquisition sequence of MSE and SE sequences than the other parameters tested. Sensitivity was about 30% higher using the SE sequence.

Figure 7: Dose-response comparison for MAGIC-f gel between SE and MSE sequences.

4. DISCUSSIONS

This study evaluated the dose sensitivity of the polymer gel MAGIC-f in a high-energy photon beam, comparing the response extracted from MSE and SE MRI sequences. In both MRI sequences, a significant difference between the initial R2 values for the first and second gel batches was identified, showing the importance of standardized polymer gel production. In this work, two different ROIs for the extraction of the R2 value: circular and 4x4 pixels. The 4 x 4 pixels ROI showed results closer to those found in the literature and was considered a better way to extract, avoiding the glass-gel interface. By avoiding this interface, the average signal intensity increases, and the measurement error decrease. Dose sensitivity values were not significantly affected comparing the two methods of analysis of the MRI. Table 2 indicates higher R2 values for the 4 x 4 pixels ROI, however, dosimetry is not affected by the choice of ROI type.

Previous studies [2] have already pointed out that gel dosimetry requires calibration of each gel batch, because minor differences in the manufacturing process and the grade of the chemical reactants influence the dosimeter's response. Our results showed that the dose-response and sensitivity were

higher for the SE MRI sequence than for MSE in accordance with previous studies using BANG gel [12]. This can be understood considering that differences between R2 values are directly associated with the magnetic resonance image acquisition process. During the MSE sequence, multiple 180° pulses in conjunction with varying phase gradient steps are applied after the 90° excitation pulse. Each 180° pulse will generate an echo, and each echo is used to fill a line in the k-space. Thus, multiple k-space rows are filled during a TR, each with distinct TE. Therefore, the TE of the image is not precisely defined in MSE as in the SE sequence, and an effective TE is assigned by the machine, which corresponds to the dominant TE for the magnitude of the imaging data (central rows of the k-space). As the process of extracting R2 or T2 is ideally connected to a series of images with well-defined TE, mapping of R2 from MSE images will suffer from greater uncertainties and a slightly reduced contrast, yielding the lower dose sensitivities observed in our measurements.

Table 3: Parameters and dose sensitivity of MAGIC-f gel published in previous studies.

	Beam Energy (MV)	Dose rate (cGy.min-1)	Field Size; SSD	Sequence / Magnetic Field	Dose sensitivity (Gy-1.s-1)
Our study	6	600	20 x 20 cm ² ; 94 cm	MSE e SE / 1.5 T	0.27 and 0.31 (MSE); 0.42 and 0.43 (SE)
Acurio, 2021	-	-	VMAT; 100 cm	MSE / 3 T	0.43
Lizar, 2021	6	-	IMRT; 100 cm	MSE / 3 T	0.43
Pavoni et al., 2017	6	-	VMAT; 100 cm	MSE / 3 T	0.36; 0.47
Resende, 2017	6	200	15 x 15 cm ² ; 100 cm	MSE / 3 T	0.35
Silveira et al., 2017	6	-	IMRT; 100 cm	MSE / 3 T	0.36; 0.37
Schwarcke, 2013	6	200	10 x 10 cm ² ; 100 cm	MSE / 3 T	0.43

Legend: SSD = source-to-surface distance; IMRT = Intensity-modulated Radiation Therapy; VMAT = Volumetric Modulated Arc Therapy; MSE = Multi Spin Echo; SE = Single Spin Echo.

We also note that for the SE MRI sequence, dose sensitivities have good agreement with previous studies, as shown in Table 2 [2, 7, 11, 13, 14, 15]. The differences between dose sensitivities found

in this study using SE sequence compared with others were lower than 22.8% (see Table 3). The dose-response linearity regime was also similar to those reported in previous studies [7, 8]. The dose sensitivity values demonstrate good agreement with those published in the literature (Table 3), with a difference of less than 28% between sequences for the greater sensitivity. One of the factors that may have influenced the variation is the dose rate dependence. The irradiation in the present work was performed at 600 cGy/min, which is different from previous studies in the literature. This dose rate was chosen because it is used more often in clinical practice.

5. CONCLUSION

The dose sensitivity values of the MAGIC-f gel indicate that the SE MRI sequence is a better choice for extracting data from R2. The importance of a calibration curve for each batch is highlighted in our study. The stochastic material variations directly influence the R2 values, which are susceptible to different conditions, such as the measurement of reagents, the manipulator that will carry out the synthesis, the concentration of trapped oxygen in test tubes, and thermal equilibrium between gel and MRI room. The MSE MRI sequence provides faster image acquisition for gel dosimetry but a distinct image contrast and dose sensitivity than the SE MRI sequence. On the other hand, the SE MRI sequence offers a more reliable and higher dose sensitivity, but at the cost of a longer acquisition time. In this study, the total time of acquiring the SE MRI sequence was almost six times larger than those of MSE for TR=3 s.

The MAGIC-f gel can be used for 3D dosimetry in irradiation procedures such as 3D, IMRT, and VMAT (Volumetric Modulated Arc Therapy), complementing the conventional forms of quality assurance (QA), establishing a benefit, and ensuring higher reliability of planned dose values. However, the clinical use requires the joint interdisciplinary collaboration between the technical staff of the MRI department to optimize the sequences, the staff responsible for the gel synthesis to ensure quality and reproducibility, and the radiation therapy team to ensure the reliability and effective use of 3D gel dosimetry.

ACKNOWLEDGMENT

This study was financed in part by the Coordenação de Aperfeiçoamento de Pessoal de Nível Superior – Brasil (CAPES) – Finance Code 001. We acknowledge the diagnostic imaging center and the radiotherapy department of Hospital São Lucas PUCRS.

REFERENCES

- [1] Baldock C, De Deene Y, Doran S, Ibbott G, Jirasek A, Lepage M, et al. Polymer gel dosimetry. *Phys Med Biol*. 2010;55(5).
- [2] Silveira MA, Pavoni JF, Baffa O. Three-dimensional quality assurance of IMRT prostate plans using gel dosimetry. *Phys Medica* [Internet]. 2017;34:1–6. Available from: <http://dx.doi.org/10.1016/j.ejmp.2016.12.007>
- [3] Pavoni JF, Pastorello BF, De Arajo DB, Baff. Formaldehyde increases MAGIC gel dosimeter melting point and sensitivity. *Phys Med Biol*. 2008;53(4).
- [4] Mather ML, Whittaker AK, Baldock C. Ultrasound evaluation of polymer gel dosimeters. *Phys Med Biol*. 2002;47(9):1449–58.
- [5] Jirasek A, Hilts M. An overview of polymer gel dosimetry using x-ray CT. *J Phys Conf Ser*. 2009;164.
- [6] De Deene Y. How to scan polymer gels with MRI? *J Phys Conf Ser*. 2010;250:69–78.
- [7] SCHWARCKE MMB. Caracterização do Gel Polimérico MAGIC-f para Aplicação em Medicina Nuclear Utilizando Imagens de Ressonância Magnética. 2013.
- [8] Pavoni JF, Baffa O. An evaluation of dosimetric characteristics of MAGIC gel modified by adding formaldehyde (MAGIC-f). *Radiat Meas*. 2012;47(11–12):1074–82.
- [9] Khan M, Heilemann G, Kuess P, Georg D, Berg A. The impact of the oxygen scavenger on the dose-rate dependence and dose sensitivity of MAGIC type polymer gels. *Phys Med Biol*. 2018;63(6).
- [10] Khan M, Heilemann G, Berg AG, Lechner W, Georg D. Basic Properties of a New Polymer Gel for 3D-Dosimetry at High Dose-Rates Typical for FFF Irradiation Based on. *Polymers* (Basel). 2019;11:E1717.
- [11] Lizar JC, Volpato KC, Brandão FC, da Silva Guimarães F, Arruda GV, Pavoni JF. Tridimensional dose evaluation of the respiratory motion influence on breast radiotherapy treatments

using conformal radiotherapy, forward IMRT, and inverse IMRT planning techniques. *Phys Medica*. 2021;81(November 2020):60–8.

[12] Maraghechi B, Gach HM, Setianegara J, Yang D, Li HH. Dose uncertainty and resolution of polymer gel dosimetry using an MRI guided radiation therapy system's onboard 0.35 T scanner. *Phys Medica* [Internet]. 2020;73(March):8–12. Available from: <https://doi.org/10.1016/j.ejmp.2020.04.004>.

[13] Acurio ESR, Lizar JC, Arruda GV, Pavoni JF. Technical Note: Three-dimensional QA of simultaneous integrated boost radiotherapy treatments by a dose-volume histogram methodology and its comparison with 3D gamma results. *Med Phys*. 2021.

[14] Pavoni JF, Neves-Junior WFP, Da Silveira MA, Haddad CMK, Baffa O. Evaluation of a composite Gel-Alanine phantom on an end-to-end test to treat multiple brain metastases by a single isocenter VMAT technique. *Med Phys*. 2017;44(9):4869–79.

[15] Resende TD. Um estudo para otimização da formulação do dosímetro gel MAGIC- f e avaliação da sua reutilização Sumário. Universidade de São Paulo; 2017.

This article is licensed under a Creative Commons Attribution 4.0 International License, which permits use, sharing, adaptation, distribution and reproduction in any medium or format, as long as you give appropriate credit to the original author(s) and the source, provide a link to the Creative Commons license, and indicate if changes were made. The images or other third-party material in this article are included in the article's Creative Commons license, unless indicated otherwise in a credit line to the material.

To view a copy of this license, visit <http://creativecommons.org/licenses/by/4.0/>.